

Cherenkov radiation of a charge flying through the inverted conical target

Andrey V. Tyukhtin ^{*}, Sergey N. Galyamin , Viktor V. Vorobev , and Aleksandra A. Grigoreva 
Saint Petersburg State University, 7/9 Universitetskaya nab., St. Petersburg, 199034 Russia

 (Received 16 April 2020; accepted 26 October 2020; published 18 November 2020)

Radiation generated by a charge moving through a vacuum channel in a dielectric cone is analyzed. It is assumed that the charge moves through the cone from the apex side to the base side (the case of inverted cone). The cone size is supposed to be much larger than the wavelengths under consideration. We calculate the wave field outside the target using the aperture method developed in our previous papers. Contrary to the problems considered earlier, here the wave which incidences directly on the aperture is not the main wave, while the wave once reflected from the lateral surface is much more important. The general formulas for the radiation field are obtained, and the particular cases of the ray-optics area and the Fraunhofer area are analyzed. Significant physical effects including the phenomenon of “Cherenkov spotlight” are discussed. In particular it is shown that the Cherenkov spotlight regime allows for reaching the most efficient radiation for the given target with the largest intensity and smallest divergence in the far-field region. Moreover, owing to the inverted cone geometry, this effect can be realized for arbitrary charge velocity, including the ultrarelativistic case, by proper selection of the cone material and the apex angle. Typical radiation patterns in the far-field area are demonstrated.

DOI: [10.1103/PhysRevA.102.053514](https://doi.org/10.1103/PhysRevA.102.053514)

I. INTRODUCTION

Cherenkov radiation (CR) produced by a moving charged particle in various complicated targets was extensively studied several decades ago in the context of development of Cherenkov detectors and counters [1,2]. Mentioned targets (or, more specifically, radiators) were typically dielectric (solid or liquid) objects like rods, cones, prisms, spheres, or their combinations. Proper manipulation with the emitted radiation (mainly for focusing purposes) was typically performed by external mirrors and lenses or, less frequently, by specific form and coating of the radiator surfaces. For example, a cylindrical radiator with the external conical mirror was utilized in the first experiments by Cherenkov [3]. Later on, conical radiators with flat or spherical end surfaces (or rods with the conical or spherical end) were considered [4–7]. The idea to form the optical surface so that the CR may be focused at a single stage of reflection or refraction also has been discussed [1]. Moreover, similar conical and prismatic targets were investigated in the context of development of radiation sources in the microwave region based on the CR effect [8,9].

In recent years, the renewed interest to the aforementioned objects has emerged. The main applications of interest are development of beam-driven radiation sources (based on high-quality beams produced by modern accelerators) and noninvasive systems for bunch diagnostics. For example, both prismatic target and hollow conical target with the flat out surface (accompanied by the set of external mirrors) have been used in a series of experiments on microwave and Terahertz CR [10–12]. The papers [11,12] should be especially noted in the context of the present paper since they used a similar

radiator. A high-power Terahertz source based on the dielectric cone having its apex facing the incident electron beam has been proposed in [11] while the paper [12] has demonstrated the first experimental results on generation of coherent CR by such a target at Kyoto University linear accelerator. A prismatic radiator (similar to that used in [8]) was proposed for CR-based bunch diagnostics in [13]. Later on, a similar prismatic target with one reflecting flat surface was discussed as a prospective candidate for simultaneous monitoring of electron and positron beams at CESR storage ring [14]. Corresponding experimental results showing the prominent possibilities of this scheme have been reported in the recent paper [15].

For further development of the discussed topics, an efficient and reliable approach is needed for analytical investigation of the CR field generated by charged particle bunches in various dielectric radiators of complex shape. Historically, various approaches, different from paper to paper, were utilized for this purpose. For example, analytical description of CR from complicated radiators of Cherenkov detectors was typically performed using the CR theory in infinite medium (Tamm-Frank theory [16,17]) and simple ray-optics laws [1,2]. In the papers [10–12] the interaction between the charge and the boundary of the target closest to the charge trajectory was taken into account semianalytically. A similar approach (taking into account only the internal target’s boundary) was used in [9] for calculation of total radiated CR energy from hollow conical radiator. In the paper [15], an exponential decay in CR intensity with an increase in the impact parameter was calculated using the so-called polarization current approximation [13]. However, all the mentioned analytical approaches do not take into account all the essential properties of radiators and the produced CR.

Starting from Ref. [18], we are developing two combined approaches which take into account both the internal radiator’s surface (which is mainly interacting with the charged

^{*}a.tyukhtin@spbu.ru

particle bunch) and the out radiator's surface (through which the CR goes into free space) [18–24]. Moreover, one of these approaches (the “aperture approach”) allows correct calculation of the CR field in the far-field (Fraunhofer) zone and near caustics formed by convergent rays where ray optics fails [20–24]. It should be underlined that though some distinct parts of these approaches were discussed and utilized earlier, their proper combinations were not collected into convenient analytical methods. It is also equally important that our approaches were successfully verified via wave simulations in COMSOL [21,22,24]. Below we briefly explain the main steps of the aperture method which is the main method for this work.

At the first step, the CR field in the bulk of the target is calculated. We suppose that this field is the same as in the corresponding etalon problem, while the latter is the problem with the medium having only the inner boundary, i.e., the boundary closest to the charged particle trajectory. It is also imposed that the etalon problem has an analytical solution. For example, for radiators with the flat surface, this is the problem with a charge moving along the plane interface between two media. Known solution of this etalon problem [25–27] was utilized in [10] and our papers [19,23]. For radiators having a cylindrical channel, this is a problem of a charge passing through a hole in an infinite dielectric medium with the solution given in [27–30]. This solution was utilized in [9] and our papers [18,20–22,24]. It is worth noting that since the etalon problem is solved rigorously, arbitrary impact parameters or channel radii (including those of order of wavelength λ) can be considered.

At the second step, we return the out boundary and select the part of it illuminated by CR (we call this part an aperture and sign it as Σ).

We assume that the radiator is large, i.e., (i) $\sqrt{\Sigma} \gg \lambda$ and (ii) the distance from the charge trajectory to Σ is large compared to λ . These assumptions allow considering CR at Σ in the form of asymptotic being the quasi-plane-wave (with small cylindrical wave front curvature). This wave can be decomposed into two orthogonal polarizations. Further the Snell and Fresnel laws can be used for calculation of the field at the outer side of the aperture.

At the third step, the aperture method utilizes Stratton-Chu formulas (also frequently called the aperture integrals) [31] to calculate the field outside the target [20–24]. Unlike the ray-optics method, this approach can be used at arbitrary wave parameter $D \sim \lambda L / \Sigma$ (L is a distance from the object and λ is a wavelength under consideration) including Fresnel area ($D \sim 1$) and Fraunhofer (far-field) one ($D \gg 1$). In addition, the aperture method is applicable in neighborhoods of caustics and focuses.

It should be noted that the aperture method does not take into account diffraction radiation (DR) generated when the charge enters and exits the target. From the physical point of view, this assumption is justified by the fact that the CR is generated over the entire path of the charge inside the target, while the DR is generated in relatively small regions near the points of entry and exit. Therefore the CR predominates the DR, and we can neglect the last one. These and other issues were discussed in more detail in our previous papers, in particular, in Refs. [22,24].

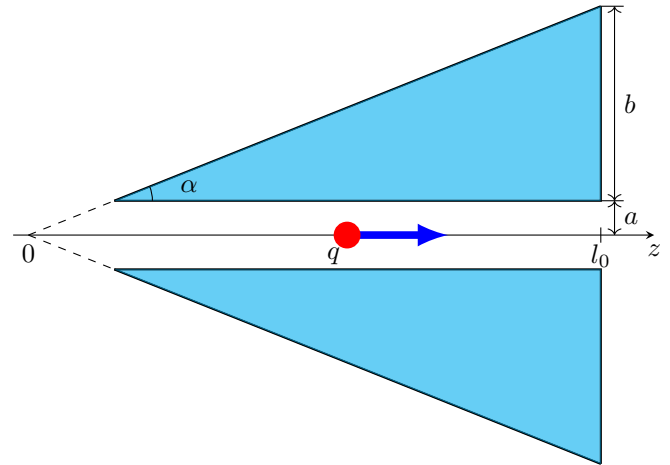


FIG. 1. The cone cross section.

This paper is devoted to the study of CR produced by a single charged particle (or a charged particle bunch) moving along the axis of the dielectric cone with the vacuum channel in the configuration similar to that in [4,11,12] (i.e., with the cone apex facing the incident charge). Throughout this paper, we will refer to this geometry as the inverted cone to clearly distinguish between this case and the analog ordinary (direct) conical target with its base facing the incident charge which was analyzed in our previous papers [18,24].

In particular, we have studied the phenomenon of the “Cherenkov spotlight” resulting in significant enhancement of CR intensity in the far-field zone [24]. However, this valuable effect takes place for certain strict limitations for the charge velocity and the cone angle only. As we will show below, in the inverted configuration considered here, corresponding conditions are much simpler to fulfill, and therefore this effect is more attractive for practical realization.

It should be noted that in this paper we mainly use the aperture method (since it is more general), however, the ray-optics solution is also derived as a specific case using the saddle point approach. Note as well that one of our main goals is to analyze the phenomenon of the Cherenkov spotlight in this situation. Therefore, the region of relatively small angles with respect to the direction of charge motion is of most importance for our analysis.

The paper is organized as follows. Section II contains solution of the etalon problem and calculation of the CR field on the aperture. The form of the aperture integrals for the problem under consideration is given in Sec. III; the particular case of the ray-optics area is considered in Sec. IV while the Fraunhofer area is considered in Sec. V. Section VI is devoted to the detailed analysis of the Cherenkov spotlight regime and Sec. VII presents the typical graphical results.

II. THE FIELD ON THE APERTURE

We analyze radiation of a charge moving along the axis of the cylindrical channel with radius a in a conical object (Fig. 1). The target is made of a material with permittivity ϵ and permeability μ (the conductivity is assumed to be negligible). The width of the ring at the cone base is b (the radius of

the cone base is $b + a$, and the cone angle is α . Accordingly, the length of the target along its axis is $l = b \cot \alpha$, and the distance from the top of the cone to its base is $l_0 = (a + b) \cot \alpha$. The target sizes are much larger than the wavelength under consideration: $b \gg \lambda$ and $l \gg \lambda$. Other restrictions on the problem parameters will be noted below.

The coordinate system origin is at the cone apex, and the z axis is the symmetry axis of the target.

The charge q moves with constant velocity $\vec{V} = c\beta\vec{e}_z$ along the z axis into the cone from the apex side. For definiteness, we will deal with a point charge having the charge density $\rho = q\delta(x)\delta(y)\delta(z - Vt)$, where δ is a Dirac delta function. However, the results obtained below can be easily generalized for the thin bunch with finite length because we consider Fourier transforms of the field components. For example, in the case of a Gaussian bunch with a charge density $\rho = q\delta(x)\delta(y)\exp[-(z - Vt)^2/(2\sigma^2)]/(\sqrt{2\pi}\sigma)$, all results for the Fourier transforms of the field components are multiplied by the factor $\exp[-\omega^2\sigma^2/(2V^2)]$, where ω is a frequency. If $\omega^2\sigma^2/(2V^2) \ll 1$ then the results for the bunch are close to those for the point charge.

It is assumed that the charge velocity exceeds the Cherenkov threshold, i.e., $\beta > 1/n$, where $n = \sqrt{\epsilon\mu} > 1$ is a refractive index of the target material. Thus, CR is generated in the cone material. Recall that CR propagates at the angle $\theta_p = \arccos(1/(n\beta))$ relative to the direction of the charge motion, coinciding with the z axis. We suppose that $\alpha < \theta_p$, i.e., the lateral (generatrix) surface of the cone is illuminated by CR. The corresponding reflected CR wave falls on the cone base and undergoes refraction here. Note that we are interested in the case when this wave does not experience the total internal reflection at the cone end surface. Naturally, Cherenkov radiation falls onto the cone base also directly, that is, without intermediate reflection from the lateral surface.

We write first the initial incident field, that is, the field in the infinite medium with the channel [22,24,27]. This field has the vertical polarization with nonzero components H_φ^{i0} , E_r^{i0} , E_z^{i0} (cylindrical coordinate system r, φ, z is used). The Fourier transform of the magnetic component at the distance $r \gg \lambda$ is

$$H_\varphi^{i0} \approx \frac{q}{c}\eta\sqrt{\frac{s}{2\pi r}} \exp\left[i\left(sr + \frac{\omega}{V}z - \frac{\pi}{4}\right)\right], \quad (1)$$

where

$$\eta = -\frac{2i}{\pi a} \left[\kappa \frac{1-n^2\beta^2}{\epsilon(1-\beta^2)} I_1(\kappa a) H_0^{(1)}(sa) + sI_0(\kappa a) H_1^{(1)}(sa) \right]^{-1}, \quad (2)$$

$s(\omega) = \frac{\omega}{V}\sqrt{n^2\beta^2 - 1}$, $\kappa(\omega) = \frac{|\omega|}{V}\sqrt{1 - \beta^2}$, $I_{0,1}$ are modified Bessel functions, $H_{0,1}^{(1)}$ are Hankel functions. Note that $\text{Im}(s(\omega)) \geq 0$ if we take into account a small dissipation. If dissipation tends to zero then this condition results in the rule $\text{sgn}[s(\omega)] = \text{sgn}(\omega)$. The result (1) is valid for $|s|r \gg 1$. The electric field \vec{E}^{i0} can be easily found because the vectors \vec{E}^{i0} , \vec{H}^{i0} and the wave vector of CR $\vec{k}_{i0} = s\vec{e}_r + \vec{e}_z\omega/V$ form the right-hand orthogonal triad in this area: $\vec{E}^{i0} =$

$-\sqrt{\mu/\epsilon}[\vec{k}_{i0}/k_{i0}, \vec{H}^{i0}]$. The angle between the wave vector \vec{k}_{i0} and the charge velocity \vec{V} is $\theta_p = \arccos[1/(n\beta)]$.

Note that the vector \vec{E} lies in the plane formed by the wave vector \vec{k} and the normal to one or another surface (the cone base or the cone lateral surface). The polarization of such a wave is usually called vertical, therefore the reflection and transmission coefficients will be supplied with the index v .

In accordance with the aperture method, we need to know the field which falls at the target's boundary being the aperture for the outer vacuum region. In the case under consideration, the aperture is the part of the cone end surface which is illuminated by CR.

First, we need to take into account the Cherenkov wave, which directly falls on the base of the cone (it can be called the first wave). The aperture for this wave is the entire base area. This wave falls on the base at the Cherenkov angle θ_p and is refracted at the angle θ_{i1} with the refraction coefficient T_{v1} :

$$\theta_{i1} = \theta_p, \quad \theta_{i1} = \arcsin(n \sin \theta_p) = \arcsin\left(\frac{\sqrt{n^2\beta^2 - 1}}{\beta}\right), \quad (3)$$

$$T_{v1} = 2\sqrt{\frac{\mu}{\epsilon}} \frac{\cos \theta_{i1}}{\sqrt{\mu/\epsilon} \cos \theta_{i1} + \cos \theta_{t1}} = 2\sqrt{\frac{\mu}{\epsilon}} \frac{1}{\sqrt{\mu/\epsilon} + n\sqrt{1 - \beta^2(n^2 - 1)}}. \quad (4)$$

Note that the effect of total internal reflection for this wave takes place under the condition $\beta^2(n^2 - 1) > 1$.

Using Eq. (1) it is easily to obtain the following expressions for the field of the first wave on the external surface of the cone base (at the point $r = r', \varphi = \varphi', z = l_0 + 0$):

$$H_{\varphi'}^{(1)}|_{z'=l_0+0} \approx Q_1 \frac{\exp(isr')}{\sqrt{kr'}} = Q_1 \frac{\exp(ikr' \sin \theta_{i1})}{\sqrt{kr'}}, \quad E_{r'}^{(1)} \approx H_{\varphi'}^{(1)} \cos \theta_{i1}, \quad E_{z'}^{(1)} \approx -H_{\varphi'}^{(1)} \sin \theta_{i1}, \quad (5)$$

where

$$Q_1 = \frac{qk\eta\sqrt{n^2\beta^2 - 1}}{c\sqrt{2\pi}\beta} T_{v1} \exp\left(\frac{ikl_0}{\beta} - \frac{i\pi}{4}\right). \quad (6)$$

Note that we took into account in (5) that the field under consideration is a quasiplane transverse wave on the almost whole aperture.

However, the first wave (5) probably is not a main wave in the important area where the angle θ is not large (in this area under certain conditions one can expect radiation which is much more intensive than at large values of angle θ). Indeed, for this wave, the angle of incidence $\theta_{i1} = \theta_p$, as a rule, is not small, and $\theta_{t1} > \theta_{i1}$. Therefore, we can expect that this wave will make a significant contribution only not for small angles θ . To describe the radiation close to the z axis, it is necessary to take into account the wave reflected from the lateral face of the cone (for brevity, we will call it the second wave; it is shown in Fig. 2). This wave can have small and even zero angles of incidence θ_{i2} and refraction θ_{t2} . Therefore this wave can be the main one in the region of relatively small angles θ .

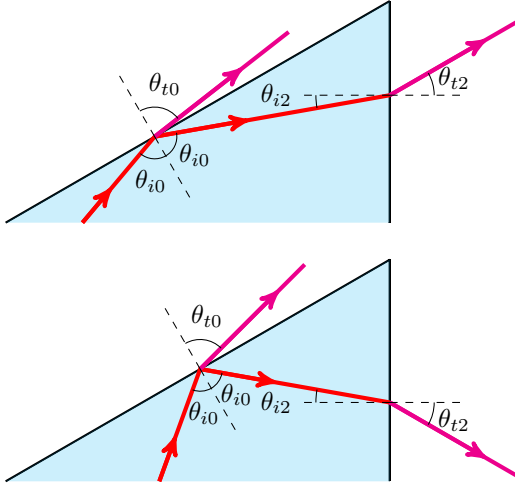


FIG. 2. The path of the ray for the case $\theta_{t2} > 0$ (top) and $\theta_{t2} < 0$ (bottom).

The initial wave (1) falls on the lateral cone boundary at the angle $\theta_{i0} = \pi/2 + \alpha - \theta_p$ (Fig. 2). It is reflected at the same angle $\theta_{r0} = \theta_{i0}$ and refracted at the angle $\theta_{t0} = \arcsin(n \sin \theta_{i0})$ with respect to the boundary normal (Fig. 2). The wave reflected from the lateral surface is the wave which incidents on the cone base (\vec{H}^{i2}). It is a cylindrical wave, as the wave (1). We can write it at the point with cylindrical coordinates r', z' in the following form:

$$H_\varphi^{i2} \approx \frac{q}{c} R_{v0} \eta \sqrt{\frac{s}{2\pi r'}} \exp[i\Phi_{i2}(r', z')], \quad (7)$$

where

$$R_{v0} = \frac{\sqrt{\mu/\varepsilon} \cos \theta_{i0} - \cos \theta_{t0}}{\sqrt{\mu/\varepsilon} \cos \theta_{i0} + \cos \theta_{t0}} \quad (8)$$

is the reflection coefficient from the lateral cone surface, and $\Phi_{i2}(r', z')$ is the phase which consists of two summands:

$$\Phi_{i2}(r', z') = \Phi_{i0}(r', z') + \Delta\Phi_i(r', z'). \quad (9)$$

Here $\Phi_{i0}(r', z')$ is the phase of the initial incident wave (1) on the lateral surface, and $\Delta\Phi_i(r', z')$ is the additional phase acquired after reflection.

For the further calculation, we need to find the point of reflection from the lateral surface. It is the solution of the system of equation for the cone generatrix and the reflected ray equation:

$$r = z \tan \alpha, \quad r = r' + (z - z') \tan \theta_{i2}, \quad (10)$$

where

$$\theta_{i2} = \theta_{r0} - (\pi/2 - \alpha) = 2\alpha - \theta_p \quad (11)$$

is the angle of incidence at the cone base (it can be easily found from Fig. 2). The solution of the system (10) is

$$r_* = z_* \tan \alpha, \quad z_* = \frac{r' - z' \tan \theta_{i2}}{\tan \alpha - \tan \theta_{i2}}. \quad (12)$$

Therefore, in accordance with (1), the phase of the initial incident wave is

$$\begin{aligned} \Phi_{i0}(r', z') &= sr_* + \frac{\omega}{V} z_* - \frac{\pi}{4} \\ &= kn \cot(\theta_p - \alpha) [r' \cos \theta_{i2} - z' \sin \theta_{i2}] - \pi/4. \end{aligned} \quad (13)$$

Additional phase $\Delta\Phi_i(r', z')$ is equal to the product of the wave number in the medium (i.e., kn) by the length of the ray:

$$\Delta\Phi_i(r', z') = kn \frac{z' - z_*}{\cos \theta_{i2}} = kn \frac{z' \sin \alpha - r' \cos \alpha}{\sin(\theta_p - \alpha)}. \quad (14)$$

Summing up (13) and (14), after simple transformation we obtain

$$\begin{aligned} \Phi_{i2}(r', z') &= kn(r' \sin \theta_{i2} + z' \cos \theta_{i2}) - \pi/4 \\ &= kr' \sin \theta_{i2} + knz' \cos \theta_{i2} - \pi/4, \end{aligned} \quad (15)$$

where θ_{t2} is the angle of refraction of the second wave on the end surface of the cone (Fig. 2):

$$\theta_{t2} = \arcsin(n \sin \theta_{i2}). \quad (16)$$

Note that we are interested only in the case when the second wave does not experience total internal reflection. It means that θ_{t2} is real, i.e., $n|\sin \theta_{i2}| < 1$.

Using (7) and (15) one can obtain the Fourier transform of the field on the external surface of the aperture (in the point with cylindrical coordinates $r', \varphi', z' = l_0 + 0$) in the following form:

$$\begin{aligned} H_{\varphi'}^{(2)}|_{z'=l_0+0} &\approx Q_2 \frac{\exp(ikr' \sin \theta_{t2})}{\sqrt{kr'}}, \\ E_r^{(2)} &\approx H_{\varphi'}^{(2)} \cos \theta_{t2}, \\ E_{z'}^{(2)} &\approx -H_{\varphi'}^{(2)} \sin \theta_{t2}, \end{aligned} \quad (17)$$

where

$$\begin{aligned} Q_2 &= \frac{q}{c} \sqrt{\frac{ks}{2\pi}} R_{v0} T_{v2} \eta e^{ikn l_0 \cos \theta_{i2} - i\pi/4} \\ &= \frac{qk \sqrt{n^2 \beta^2 - 1}}{c \sqrt{2\pi \beta}} R_{v0} T_{v2} \eta e^{ikn l_0 \cos \theta_{i2} - i\pi/4}, \end{aligned} \quad (18)$$

and T_{v2} is the coefficient of refraction:

$$T_{v2} = \frac{2\sqrt{\mu/\varepsilon} \cos \theta_{i2}}{\sqrt{\mu/\varepsilon} \cos \theta_{i2} + \cos \theta_{t2}}. \quad (19)$$

Concluding this section, we should note that for $\theta_{i2} < 0$, there is also another way for the second wave to reach the output surface: it can be reflected from the far cone generatrix. In other words, if we look at Fig. 1, the wave falls on the lower lateral face, reflects from it, passes through the axis of the structure and falls on the base of the cone. However, such a path of the wave propagation is associated with diffraction of the wave by the channel, which cannot be described by simple ray-optics laws. We will neglect this pass of propagation. This can be done if the negative angle of incidence is sufficiently small: $\theta_{i2} < 0$ but $|\theta_{i2}| \ll \alpha$. It is easy to show that, under this condition, the part of the base illuminated by this wave is relatively small. This limitation is not very important for our main goal, which is to analyze the radiation at not big angles θ , where, under certain conditions, we hope to get radiation much more intense than in other directions. Note that, in the case of positive angle θ_{i2} , such a restriction does not occur.

III. APERTURE INTEGRALS FOR THE INVERTED CONE

Now we should write the general Stratton-Chu formulas [see Eq. (1) from Ref. [24]] in the form which is convenient for further calculation in the case of the considered target. Because of axial symmetry of the problem we can place the observation point in the plane $y = 0$, then $\vec{e}_r = \vec{e}_x$, $\vec{e}_\varphi = \vec{e}_y$. As well, we take into account that the normal to the aperture coincides with the z axis: $\vec{n}' = \vec{e}_z$. We will use further the following formulas:

$$\tilde{R} = |\vec{R} - \vec{R}'| = \sqrt{r^2 + r'^2 - 2rr' \cos \varphi' + (z - l_0)^2}, \quad (20)$$

$$[\vec{n}' \times \vec{H}(\vec{R}')] = -H_{\varphi'}(\vec{R}')(\vec{e}_r \cos \varphi' + \vec{e}_\varphi \sin \varphi'), \quad (21)$$

$$\nabla' G(\vec{R}) = \left(\vec{e}_{r'} \partial_{r'} + \frac{\vec{e}_{\varphi'}}{r'} \partial_{\varphi'} + \vec{e}_z \partial_{z'} \right) G(\vec{R}), \quad (22)$$

$$\begin{aligned} [\vec{n}' \times \vec{E}(\vec{R}')] &= [\vec{e}_z \times \vec{e}_{r'}] H_{\varphi'}(\vec{R}') \cos \theta_{tm} \\ &= \vec{e}_{\varphi'} H_{\varphi'}(\vec{R}') \cos \theta_{tm}, \end{aligned} \quad (23)$$

$$\begin{aligned} [[\vec{n}' \times \vec{E}(\vec{R}')] \times \nabla'] G(\vec{R}) &= H_{\varphi'}(\vec{R}') \cos \theta_{tm} \\ &\times [\vec{e}_{r'} \partial_{z'} - \vec{e}_z \partial_{r'}] G(\vec{R}), \end{aligned} \quad (24)$$

where m is the number of the wave exiting the target ($m = 1, 2$). Here, for brevity, we introduce the notation for the partial derivative: $\partial_x \equiv \partial/\partial x$ (further, analogously, the second derivative is written in the form $\partial_{xy} \equiv \frac{\partial^2}{\partial x \partial y}$).

Using (20) and (24), after a series of cumbersome transformations, one can obtain from Stratton-Chu formulas [Eq. (1) from Ref. [24]] the following result for the m th part of the field generated by the wave with number m :

$$\begin{aligned} E_{\varphi}^{(m)} &= 0, \\ \begin{Bmatrix} E_r^{(m)} \\ E_z^{(m)} \end{Bmatrix} &= -\frac{i}{2\pi k} \int_{r_{ml}}^{r_{mh}} dr' \int_0^\pi d\varphi' r' H_{\varphi'}^{(m)}(\vec{R}') \\ &\times \left\{ \begin{aligned} &k^2 \cos \varphi' + \cos \varphi' \cdot \partial_{r'r'} + \frac{\sin \varphi'}{r'^2} \cdot \partial_{\varphi'} - \frac{\sin \varphi'}{r'} \cdot \partial_{r'\varphi'} + ik \cos \theta_{tm} \cos \varphi' \cdot \partial_{z'} \\ &\partial_{z'r'} - ik \cos \theta_{tm} \cdot \partial_{r'} \end{aligned} \right\} G(\vec{R}), \end{aligned} \quad (25)$$

where m is a number of the considered wave, and θ_{tm} is the corresponding angle of refraction. Note that obtaining the result of (25), we used the properties of the evenness and oddness of various terms in the integrands (in particular, this leads to zeroing $E_{\varphi}^{(m)}$). The total radiation field is the sum of these components: $\vec{E} \approx \sum_m \vec{E}^{(m)}$.

The integration limits r_{ml} , r_{mh} are determined by the limits of the aperture, that is, the cone base part which is illuminated by the wave under consideration. For two waves under consideration,

$$\begin{aligned} r_{1l} &= a, \\ r_{2l} &= \max(a, a + l \tan \theta_{i2}), \\ r_{1h} &= r_{2h} = a + b. \end{aligned} \quad (26)$$

The formula for r_{2l} is explained by the fact that the illuminated part of the cone base is smaller than the entire base in the case of $\theta_{i2} > 0$.

Note that we integrate over the entire illuminated part of the cone base, from the channel boundary to the lateral surface of the cone. Here we neglect the fact that the field is not determined by the ray-optics laws in the vicinities of these extreme points. This is explained by the fact that sizes of these vicinities are of the order of the wavelength. Therefore, the relative error in integrals (25) is of the order of $(kb)^{-1}$. Such a value can be neglected because the theory is constructed just with such accuracy.

Further one can exactly find all derivatives in (25), but the result will be very cumbersome. On the other hand, the exact calculation is not very important, because, as a rule, we are interested in the field on the distance much larger than wavelength under consideration. Assuming that $k|z - l_0| \gg 1$ and, therefore, $k\tilde{R} \gg 1$ for all values of r' , φ' , we can differentiate only $\exp(ik\tilde{R})$ in the function $G(\vec{R})$. As a result, the formulas (25) are reduced to the following one:

$$\begin{Bmatrix} E_r^{(m)} \\ E_z^{(m)} \end{Bmatrix} = -\frac{ik}{2\pi} \int_{r_{ml}}^{r_{mh}} dr' \int_0^\pi d\varphi' r' H_{\varphi'}^{(m)}(\vec{R}') \frac{e^{ik\tilde{R}}}{\tilde{R}^3} \left\{ \begin{aligned} &(z - l_0)^2 \cos \varphi' + rr' \sin^2 \varphi' + (z - l_0)\tilde{R} \cos \theta_{tm} \cos \varphi' \\ &(r' - r \cos \varphi')(\tilde{R} \cos \theta_{tm} + z - l_0) \end{aligned} \right\}. \quad (27)$$

Using the expressions (5) and (17) for $H_{\varphi'}^{(m)}$ we obtain

$$\begin{Bmatrix} E_r^{(m)} \\ E_z^{(m)} \end{Bmatrix} = -\frac{iQ_m}{2\pi} \int_{r_{ml}}^{r_{mh}} dr' \int_0^\pi d\varphi' \frac{\sqrt{kr'} e^{i\Phi_m(r', \varphi')}}{\tilde{R}^3} \left\{ \begin{aligned} &(z - l_0)^2 \cos \varphi' + rr' \sin^2 \varphi' + (z - l_0)\tilde{R} \cos \theta_{tm} \cos \varphi' \\ &(r' - r \cos \varphi')(\tilde{R} \cos \theta_{tm} + z - l_0) \end{aligned} \right\}, \quad (28)$$

where

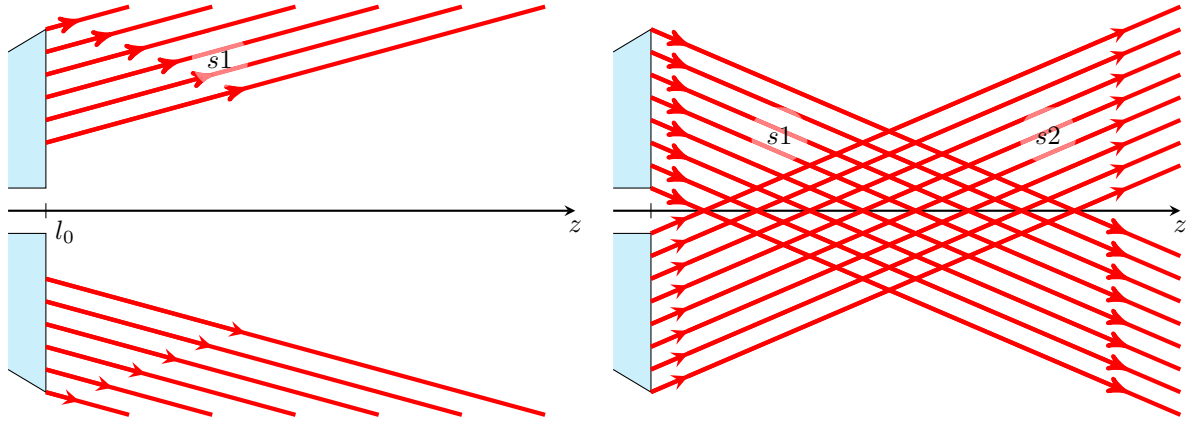
$$\Phi_m(r', \varphi') = kr' \sin \theta_{tm} + k\tilde{R}(r', \varphi'). \quad (29)$$

IV. RAY-OPTICS APPROXIMATION

Let us find the saddle point (or stationary phase point) for the integrands in (28). This point is determined by equa-

tions [32],

$$\frac{\partial \Phi_m(r', \varphi')}{\partial r'} = 0, \quad \frac{\partial \Phi_m(r', \varphi')}{\partial \varphi'} = 0. \quad (30)$$


 FIG. 3. The ray picture outside the cone in the cases of $\theta_{t2} > 0$ (left) and $\theta_{t2} < 0$ (right).

It is easily to find that this system has the following two solutions:

$$\begin{aligned} r' &= r_m^{s1} = r - (z - l_0) \tan \theta_{tm}, & \varphi' &= \varphi_m^{s1} = 0; \\ r' &= r_m^{s2} = -r - (z - l_0) \tan \theta_{tm}, & \varphi' &= \varphi_m^{s2} = \pi. \end{aligned} \quad (31)$$

Since $\theta_{t1} > 0$, then $r_1^{s2} < 0$, and this saddle point lies beyond the integration limits. Therefore the first wave is determined only by the saddle point $s1$ with $r' = r_1^{s1}$. At the same time, the value θ_{t2} can be both positive and negative. Therefore both saddle points $s1, 2$ can be significant for the second wave. First of all, we consider this wave.

Simple transformations give the following expressions for \tilde{R} and Φ_2 in the saddle points:

$$\tilde{R}(r_2^{s1}, \varphi_2^{s1}) = \tilde{R}(r_2^{s2}, \varphi_2^{s2}) = (z - l_0) / \cos \theta_{t2}, \quad \Phi_2^{s1,2} = \Phi_2(r_2^{s1,2}, \varphi_2^{s1,2}) = k[\pm r \sin \theta_{t2} + (z - l_0) \cos \theta_{t2}]. \quad (32)$$

Further we will need as well values of the second derivatives of the phase in the saddle points:

$$\left. \frac{\partial^2 \Phi_2}{\partial r'^2} \right|_{s1,2} = k \frac{\cos^3 \theta_{t2}}{z - l_0}, \quad \left. \frac{\partial^2 \Phi_2}{\partial \varphi'^2} \right|_{s1,2} = \pm \frac{r r_2^{s1,2} \cos \theta_{t2}}{z - l_0}, \quad \left. \frac{\partial^2 \Phi_2}{\partial \varphi' \partial r'} \right|_{s1,2} = 0. \quad (33)$$

We can approximately calculate the integrals (28) by the stationary phase method if the aperture contains a large number of Fresnel zones, in other words, the function $e^{i\Phi_2(r', \varphi')}$ experiences a large number of oscillations within this area. This condition means that $|\Phi_2(r', \varphi') - \Phi_2^{s1,2}| \gg 1$ on the most part of the aperture. We can write this inequality as $|\frac{\partial^2 \Phi_2}{\partial r'^2} b^2| \gg 1$. If $\cos \theta_{t2}$ is not very small, then we obtain $|\frac{kb^2}{z-l_0}| \gg 1$, or

$$D \sim \frac{\lambda(z - l_0)}{\pi b^2} \ll 1. \quad (34)$$

The parameter D is usually called a wave parameter [33]. The inequality (34) is the condition of applicability of the ray-optics approximation.

Applying the known expression for asymptotic of double integral [32] one can obtain the following result:

$$\begin{aligned} \vec{E}^{(2)} &\approx \vec{E}^{s1} + \vec{E}^{s2}, \\ \begin{cases} E_r^{s1} \\ E_z^{s1} \end{cases} &= Q_2 \frac{e^{i\Phi_2^{s1}}}{\sqrt{kr}} \begin{cases} \cos \theta_{t2} \\ -\sin \theta_{t2} \end{cases} \begin{cases} 1 & \text{for } r_{2l} < r - (z - l_0) \tan \theta_{t2} < r_{2h}, \\ 0 & \text{otherwise} \end{cases}, \\ \begin{cases} E_r^{s2} \\ E_z^{s2} \end{cases} &= Q_2 \frac{e^{i\Phi_2^{s2}}}{\sqrt{kr}} \begin{cases} \cos \theta_{t2} \\ \sin \theta_{t2} \end{cases} \begin{cases} 1 & \text{for } -r_{2h} < r + (z - l_0) \tan \theta_{t2} < -r_{2l}, \\ 0 & \text{otherwise} \end{cases}, \end{aligned} \quad (35)$$

where

$$\Phi_2^{s1} = kr \sin \theta_{t2} + k(z - l_0) \cos \theta_{t2}, \quad \Phi_2^{s2} = -kr \sin \theta_{t2} + k(z - l_0) \cos \theta_{t2} - \pi/2. \quad (36)$$

One can see that the contributions of stationary points exist only in certain regions shown in Fig. 3 (their borders are ray-optics boundaries). These limitations are explained by the fact that only under such conditions the stationary phase points are in the limits of integration (on the aperture), i.e.,

$r_{2l} < r_2^{s1,2} < r_{2h}$. If this condition is violated for one of the stationary points, then this point is outside the aperture, and its contribution is zero. More precisely one can say that the ray-optics solution (35) is suitable at some distance from the ray-optics boundaries exceeding the wavelength.

Equation (35) describes two quasi-plane-waves (more precisely, they are cylindrical waves with small curvature of the constant phase surface). Naturally, these waves are transverse because the projections on the propagation direction are zero: $E_{\parallel}^{s1,2} = \pm E_r^{s1,2} \sin \theta_{t2} + E_z^{s1,2} \cos \theta_{t2} = 0$. The electric field is orthogonal to the propagation direction:

$$E_{\perp}^{s1,2} = H_{\varphi}^{s1,2} = Q_2 \exp(i\Phi_2^{s1,2})/\sqrt{kr}. \quad (37)$$

The wave “s1” exists for any sign of the angles θ_{t2}, θ_{t2} and propagates at the angle θ_{t2} with respect to the z axis (Fig. 3, left and right). The wave “s2” exists only in the case $\theta_{t2}, \theta_{t2} < 0$ and propagates at the angle $|\theta_{t2}| = -\theta_{t2}$ with respect to the z axis (Fig. 3, right). Note that in the case $\theta_{t2}, \theta_{t2} < 0$ (that is, $2\alpha < \theta_p$), the rays converge to the z axis, and there is a certain rhomboidal area where the rays are intersected (Fig. 3, right). In this area, the ray-optics solution (35) tends to infinity if $r \rightarrow 0$ on the segment $r_{2l}/\tan|\theta_{t2}| < z - l_0 < r_{2h}/\tan|\theta_{t2}|$. This means that the ray-optics approximation is not applicable at distances from the z axis less than the wavelength under consideration. However, we can expect that the real field has a large value in this area.

Naturally, the expressions (35) can be obtained with help of the ray-optics method [33,34]. Let us give this derivation briefly. The wave exiting the target is a quasiplane transversal wave having the electric and magnetic fields equal each other and determined by the formula (17) on the aperture. Because of axial symmetry the exiting wave is cylindrical. Considering also that the boundary of the object in its section is a straight line, it is easy to conclude that the wave amplitude in the point (r, z) differs from one in the point (r', l_0) only by replacement r' to r (similar effect is discussed in [18] for other objects). Thus the formula (17) results in the expression $|E^{(2)}| = |Q_2|/\sqrt{kr}$ which corresponds to Eq. (35).

It remains to determine the phases of two waves. First we consider the wave “s1” radiated from the upper part of the aperture. Taking into account that the length of the ray outside the target is $(z - l_0)/\cos \theta_{t2}$ we have for the phase at the point (r, z) ,

$$\Phi_2(r, z) = \Phi_{i2}(r', l_0) + k \frac{z - l_0}{\cos \theta_{t2}}, \quad (38)$$

where $\Phi_{i2}(r', l_0)$ is given by the formula (15) with $r' = r - (z - l_0) \tan \theta_{t2}$. Substituting (15) in (38) one can obtain that

$$\begin{aligned} \Phi_2(r, z) &= k[nl_0 \cos \theta_{t2} + r \sin \theta_{t2} + (z - l_0) \cos \theta_{t2}] \\ -\pi/4 &= \arg Q_2 + \Phi_2^{s1}, \end{aligned} \quad (39)$$

which corresponds to (35) and (36).

A similar way gives a corresponding result for the wave “s2” if we take into account that for this wave $\theta_{t2} < 0$. However, we should take into account the following difference. The ray “s2” passes through the z axis, which is a caustic where the ray tube cross section tends to zero. It is known [33] that during the passage of the caustic, the phase of the wave changes to $\pi/2$. Taking into account this factor, we obtain $\Phi_2(r, z) = \arg Q_2 + \Phi_2^{s2}$, where Φ_2^{s2} is given by Eq. (36).

Until now in this section, we have considered only the second wave (that is, the wave reflected from the lateral boundary). The ray-optical analysis of the first wave is simpler, since it is determined by one saddle point “s1” only. By analogy with formulas (35), we obtain

$$\begin{aligned} \vec{E}^{(1)} &\approx \vec{E}^{s1} + \vec{E}^{s2}, \\ \begin{Bmatrix} E_r^{s1} \\ E_z^{s1} \end{Bmatrix} &= Q_1 \frac{e^{i\Phi_1^{s1}}}{\sqrt{kr}} \begin{Bmatrix} \cos \theta_{t1} \\ -\sin \theta_{t1} \end{Bmatrix} \\ &\times \begin{cases} 1 & \text{for } r_{1l} < r - (z - l_0) \tan \theta_{t1} < r_{1h} \\ 0 & \text{otherwise} \end{cases}, \end{aligned} \quad (40)$$

where

$$\Phi_1^{s1} = kr \sin \theta_{t1} + k(z - l_0) \cos \theta_{t1}. \quad (41)$$

V. FRAUNHOFER AREA

Now we consider the area where the wave parameter is large: $D \gg 1$. Usually this area is named Fraunhofer, or far-field, area. Corresponding asymptotic can be obtained from both general approximate formulas [see Eq. (5) from Ref. [24]] and the expressions (28) obtained for the geometry under consideration.

Based on Eq. (28), we can use the approximation $\tilde{R} \approx R_0(1 - rr' \cos \varphi' R_0^{-2})$ (here $R_0 = \sqrt{r^2 + (z - l_0)^2}$) in the phase $\Phi_m(r', \varphi')$ and rougher approximation $R \approx R_0$ in other factors in the integrand:

$$\begin{Bmatrix} E_r^{(m)} \\ E_z^{(m)} \end{Bmatrix} = -\frac{iQ_m}{2\pi} \frac{e^{ikR_0}}{R^3} (R \cos \theta_{tm} + z) \begin{Bmatrix} z \\ -r \end{Bmatrix} \int_{r_{ml}}^{r_{mh}} dr' \int_0^\pi d\varphi' \sqrt{kr'} \cos \varphi' \exp\left(-ik \frac{r}{R_0} r' \cos \varphi' + ikr' \sin \theta_{tm}\right). \quad (42)$$

Further it is convenient to use spherical coordinates R, θ (counted from the z axis), and φ (counted from the x axis). Using the formulas,

$$E_R = E_r \sin \theta + E_z \cos \theta, \quad E_\theta = E_r \cos \theta - E_z \sin \theta, \quad (43)$$

one can obtain $E_R^{(m)} = 0$ and

$$E_\theta^{(m)} = -\frac{iQ_m}{2\pi} \frac{e^{ikR_0}}{R} (\cos \theta_{tm} + \cos \theta) \int_{r_{ml}}^{r_{mh}} dr' \sqrt{kr'} I_1(\chi) e^{ikr' \sin \theta_{tm}}, \quad (44)$$

where

$$I_1(\chi) = \int_0^\pi e^{-i\chi \cos x} \cos x dx,$$

and $\chi = kr'rR_0^{-1} \approx kr' \sin \theta$. The integral $I_1(\chi)$ is known and expressed in terms of the Bessel function $J_1(\chi)$ [35]:

$$I_1(\chi) = -\pi i J_1(\chi). \quad (45)$$

Asymptote of this function for $\chi \gg 1$ is

$$I_1(\chi) \approx -i \sqrt{\frac{2\pi}{\chi}} \cos\left(\chi - \frac{3\pi}{4}\right), \quad (46)$$

and the error has the order of $O(\chi^{-3/2})$.

If the condition $kb\theta \gg 1$ is true then $kr' \sin \theta \gg 1$ on the almost whole aperture, and using (46) we obtain from (44) the following result:

$$E_\theta^{(m)} \approx H_\varphi^{(m)} \approx -\frac{Q_m}{\sqrt{2\pi}} \frac{\cos \theta + \cos \theta_{tm}}{\sqrt{\sin \theta}} F_m(\theta) \frac{d_m}{R} e^{ikR_0}, \quad (47)$$

where

$$\begin{aligned} F_m(\theta) &= \frac{1}{d_m} \int_{r_{ml}}^{r_{mh}} \cos\left(kr' \sin \theta - \frac{3\pi}{4}\right) \exp(ikr' \sin \theta_{tm}) dr' \\ &= \frac{\sin(d_m w_{m-})}{d_m w_{m-}} e^{i\bar{r}_m w_{m-} + 3i\pi/4} \\ &\quad + \frac{\sin(d_m w_{m+})}{d_m w_{m+}} e^{i\bar{r}_m w_{m+} - 3i\pi/4}, \end{aligned} \quad (48)$$

$$w_{m\pm} = k(\sin \theta_{tm} \pm \sin \theta),$$

$$d_m = \frac{r_{mh} - r_{ml}}{2}, \quad \bar{r}_m = \frac{r_{mh} + r_{ml}}{2}. \quad (49)$$

$$d_1 = b/2, \quad \bar{r}_1 = b/2 + a,$$

$$d_2 \approx \begin{cases} (b - l \tan \theta_{i2})/2 & \text{for } \theta_{i2} > 0, \\ b/2 & \text{for } \theta_{i2} < 0, \end{cases}$$

$$\bar{r}_2 = \begin{cases} a + (b + l \tan \theta_{i2})/2 & \text{for } \theta_{i2} > 0, \\ a + b/2 & \text{for } \theta_{i2} < 0. \end{cases}$$

The radiation pattern is determined primarily by the function $F_m(\theta)$. Since $\theta_{i1} > 0$ then the function $F_1(\theta)$ has the main maximum at $\theta = \theta_{i1}$ [in fact, only the first summand in (48) has the importance for the function $F_1(\theta)$].

The behavior of the function $F_2(\theta)$ is more complex. If $\theta_{i2} > 0$ then the main maximum of the function $F_2(\theta)$ is determined by the first summand in (48): It takes place for $\theta = \theta_{i2}$ (radiation comes mainly from the upper part of the aperture, as it is shown in the left plot of Fig. 2). If $\theta_{i2} < 0$ then the main maximum of the function $F_2(\theta)$ is determined by the second summand in (48): It takes place for $\theta = -\theta_{i2} = |\theta_{i2}|$ (radiation comes mainly from the lower part of the aperture, as it is shown in the right plot of Fig. 2).

Thus, the direction of maximal radiation coincides with the direction of the refraction wave (this is natural). In any case, the maximum values of $|F_m(\theta)|$ is approximately equal to 1, and maxima of the fields are equal to

$$|E_\theta^{(m)}|_{\max} \approx \frac{|Q_m|}{\sqrt{2\pi}} \frac{2 \cos \theta_{tm}}{\sqrt{\sin \theta_{tm}}} \frac{d_m}{R}. \quad (50)$$

The angular width $\delta\theta$ of the main lobes of the diagrams is $\delta\theta \approx \frac{2\pi}{kd \cos \theta_{tm}}$.

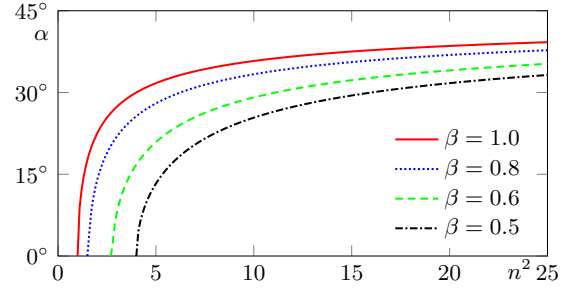


FIG. 4. The cone angle for the Cherenkov spotlight effect depending on the refractive index square $n^2 = \varepsilon\mu$ for different values of the charge velocity.

Recall that expressions for Q_m are determined by Eqs. (6) and (18). Assuming that angles θ_{tm} are not close to 0 or $\pi/2$ and β is not small, we can give the following rough estimation for the maximal field values:

$$|E_\theta^{(m)}|_{\max} \sim |Q_m| \frac{d_m}{R} \sim \frac{|qk\eta|}{c} \frac{b}{R}. \quad (51)$$

Note that this estimation is true as well for other objects if we consider b as some characteristic size of the aperture. For example, in the case of the infinite plate, the value b is the radius of the illuminated area of the plate surface, and in the case of the direct cone the value b is the length of the illuminated part of the lateral surface [24]. However, this rule has an important exception which is discussed below.

VI. CHERENKOV SPOTLIGHT

Note that the expressions (47) and (48) are not true for $kb\theta \leq 1$. However, this angle range is very interesting in the important case when the second wave propagates along the symmetry axis that is $\theta_{i2} = \theta_{r2} = 0$ (for the first wave this situation is impossible). According to (11), this situation takes place when

$$\alpha = \frac{\theta_p}{2} = \arccos((n\beta)^{-1})/2. \quad (52)$$

Figure 4 shows dependency of the cone angle (52) on the refractive index for different values of the charge velocity. Let us consider this case separately, assuming, as in the previous section, that the observation point is in the Fraunhofer region ($D \gg 1$).

The integrand in (44) contains the Bessel function, which can be represented in the form of the Taylor series [36]. After that, in the case $\theta_{i2} = \theta_{r2} = 0$ we obtain

$$E_\theta^{(2)} = -\frac{Q_2}{2} \frac{e^{ikR_0}}{R} \int_{r_{2l}}^{r_{2h}} U(r') dr', \quad (53)$$

where $r_{2l} = a$, $r_{2h} = a + b \approx b$,

$$U(r') = \sum_{j=0}^{\infty} \frac{(-1)^j (\sin \theta)^{2j+1}}{2^{2j} j! (j+1)!} (kr')^{2j+3/2}. \quad (54)$$

Calculating the integrals of the terms of the series and considering that $a \ll b$, we obtain the following result:

$$E_\theta^{(2)} = -\frac{Q_2}{5} (kb)^{3/2} F_0(\theta) \frac{e^{ikR_0}}{kR}, \quad (55)$$

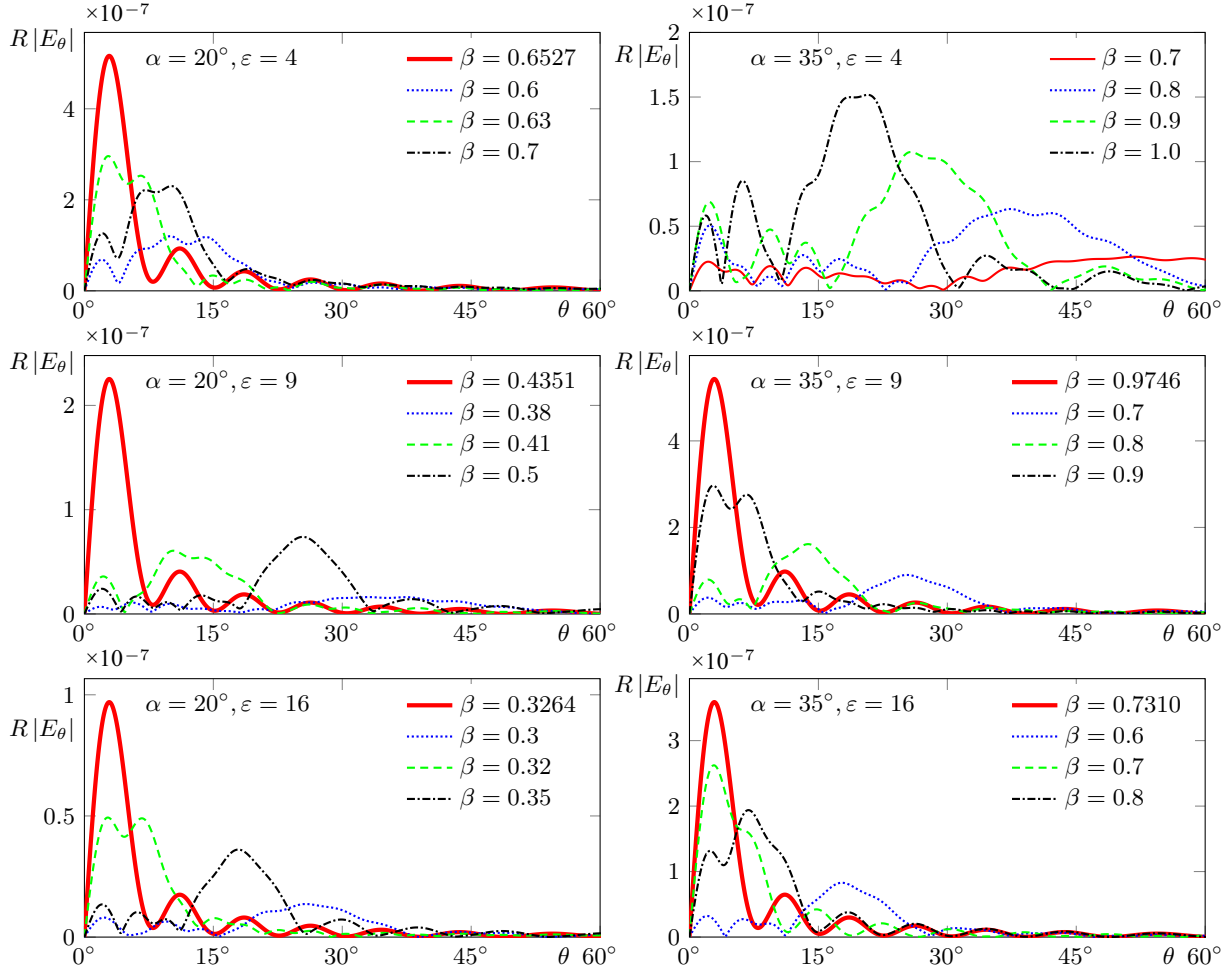


FIG. 5. The angular distribution of the magnitude of the electric field Fourier transform in the Fraunhofer area (in units V s). Parameters are as follows: $a = c/\omega, b = 50c/\omega = 50/k, q = 1 \text{ nC}, \mu = 1$; the cone angle α and the charge velocity β are indicated in the plots.

where

$$F_0(\theta) = \sum_{j=0}^{\infty} \frac{(-1)^j (kb \sin \theta)^{2j+1}}{(4j/5 + 1)2^{2j} j! (j+1)!}. \quad (56)$$

Taking into account that $kb \sin \theta \leq 1$ one can obtain the simple approximation,

$$F_0(\theta) \approx kb\theta \left[1 - \frac{5}{72} (kb\theta)^2 \right]. \quad (57)$$

The angle of the maximum θ_{\max} and the maximal value of this function can be estimated as

$$\theta_{\max} \sim 1/(kb), \quad F_{0\max} \sim 1. \quad (58)$$

Comparing the maximal value of the field in the case $\theta_{i2} = 0$ and in the case $\theta_{i2} \sim 1$ one can obtain

$$\frac{|E_{\theta}^{(2)}|_{\max}|_{\theta_{i2}=0}}{|E_{\theta}^{(2)}|_{\max}|_{\theta_{i2}\sim 1}} \sim \frac{\sqrt{2\pi}}{10} \frac{\sqrt{\sin \theta_{i2}}}{\cos \theta_{i2}} F_{0\max} \frac{(kb)^{3/2}}{kd_2} \sim \sqrt{kb} \gg 1. \quad (59)$$

Thus, if $\theta_{i2} = 0$, then the field maximum is located at the small angle (58), and its value is much larger than that for $\theta_{i2} \sim 1$. Such an effect can be called the Cherenkov spotlight.

Note that the similar phenomenon occurs also for the case when the charge flies into the cone from the side of its base (the direct cone) [24]. However, there is strong difference of conditions for reaching the effect. For the direct cone, the spotlight effect is possible only in a certain very narrow range of charge velocities close to the speed of light in the medium [24]. In the case of the inverted cone, this effect can be achieved for any charge velocity $\beta > 1/n$ due to the proper selection of the cone angle α or refractive index n in accordance with the condition (52).

It is especially important that the Cherenkov spotlight regime is easily reachable for the ultrarelativistic charge with $\beta \approx 1$ (recall that this is impossible for the direct cone). Note as well that the essential advantage of the inverted cone is the fact that the Cherenkov spotlight effect is not very sensitive to the selection of the cone parameters (as can be seen from Fig. 4, for the case $\beta = 1$, the dependence of the corresponding angle α on the refractive index square is rather weak for $n^2 > 5$).

VII. NUMERICAL RESULTS

Figure 5 demonstrates results of computation of the field in the far-field (Fraunhofer) area. These results have been

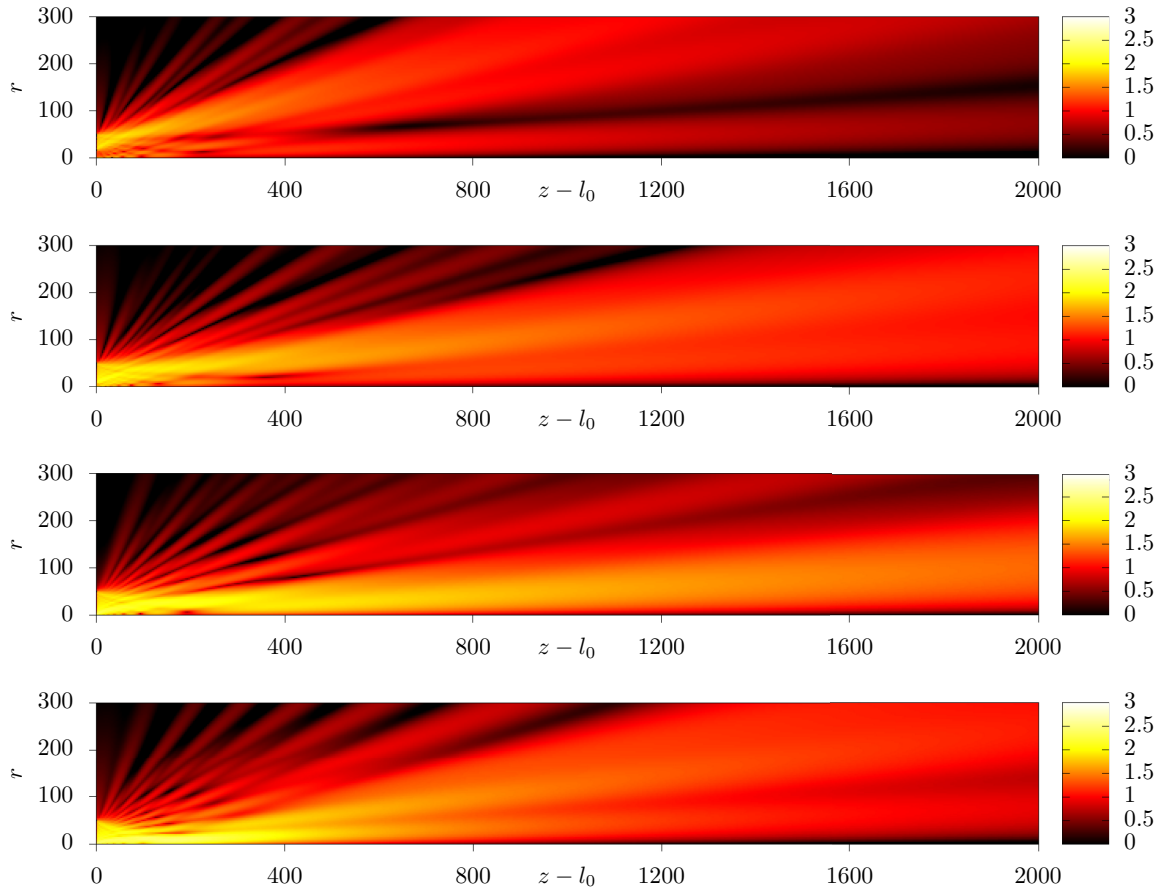


FIG. 6. Distribution of the electric field in the space for the following parameters: $\varepsilon = 4$, $\mu = 1$, $\alpha = 20^\circ$, $a = c/\omega$, $b = 50c/\omega$, $q = 1$ nC; $\beta = 0.6$ (top plot), $\beta = 0.63$ (second plot), $\beta = 0.6527$ (third plot), $\beta = 0.7$ (bottom plot). Distances are given in c/ω units. The module of Fourier transform of the electric field is given in logarithmic scale and normalized by 10^{-9} V/m s (the level “0”).

obtained with use of formula (44) which allows calculating the field everywhere in this region including the region of small angles θ (therefore the Cherenkov spotlight effect can be analyzed in this way).

Figure 5 shows the angle dependency of the module of the Fourier transform of the field for different values of the cone angle α and the cone material permittivity ε (it is assumed that $\mu = 1$). The vertical axis on the plots shows the value $R|E_\theta|$ which does not depend on the distance R in the Fraunhofer area.

Each plot contains four curves. For the bold red solid curve, the charge velocity corresponds to the condition (52) (i.e., $\theta_{t2} = 0$) determining the Cherenkov spotlight effect. Other curves correspond to the cases when $\theta_{t2} \neq 0$. One can see that the maximal field value is much larger for the spotlight case compared to the cases when velocities differ essentially from the spotlight velocity. It is also notable that such an effect cannot be reached for the case where $\alpha = 35^\circ$, $\varepsilon = 4$ (as one can see from Fig. 4, if $n^2 = 4$ then this effect can be realized only for $\alpha < 30^\circ$).

For all other parameters indicated in Fig. 5, the spotlight velocity can be found and therefore the spotlight effect can be realized.

Note as well that approximate expressions (47) (for the case when θ_t is not small) and (55) and (57) (for the case of

the Cherenkov spotlight when $\theta_t = 0$) give good coincidence with the results shown in Fig. 5 (the discrepancy in the areas of the high field values does not exceed a few percent).

Figure 6 shows two-dimensional distribution of the electric field of CR calculated with aperture integrals (27) and (28) which cover the ray-optics area, the Fresnel area, and the Fraunhofer area. The plots illustrate the cases shown in the first plot of Fig. 5. One can clearly see the Cherenkov spotlight effect for the charge velocity $\beta = 0.6527$. In this case the main maximum lies at minimal angle θ , and its value is maximal. In all other cases the radiation is dissipated essentially stronger.

VIII. CONCLUSION

We have studied the radiation generated by a charge moving in a vacuum channel through the “inverted” dielectric cone assuming that the cone sizes are much larger compared to the wavelengths of interest. The wave field outside the target was calculated using the aperture method developed in our previous papers.

It is worth noting that contrary to the problems considered earlier, here the wave which incidences directly on the aperture is not the main wave, while the wave once reflected from the lateral surface is much more important. We have obtained

the analytical results for CR outside the target (including the ray-optics area and the most interesting Fraunhofer area) and analyzed significant physical effects.

The most promising effect is the Cherenkov spotlight phenomenon which allows reaching essential enhancement of the CR intensity in the far-field region at certain selection of the problem parameters (the field in the main maximum can be increased approximately in \sqrt{kb} times). It is important as well that for the inverted cone geometry, this effect can be realized

for arbitrary charge velocity, including the case $\beta \approx 1$, by proper selection of the cone material and the apex angle. This is one of the important advantages of the inverted cone because this phenomenon is unattainable for the ultrarelativistic bunch in the case of the direct cone [24].

ACKNOWLEDGMENT

This research was supported by the Russian Science Foundation, Grant No. 18-72-10137.

-
- [1] J. V. Jelley, *Čerenkov Radiation and its Applications* (Pergamon, Oxford, 1958).
- [2] V. P. Zrellov, *Vavilov-Cherenkov Radiation in High-Energy Physics* (Israel Program for Scientific Translations, Jerusalem, 1970).
- [3] P. A. Čerenkov, *Phys. Rev.* **52**, 378 (1937).
- [4] I. A. Getting, *Phys. Rev.* **71**, 123 (1947).
- [5] R. H. Dicke, *Phys. Rev.* **71**, 737 (1947).
- [6] J. Marshall, *Phys. Rev.* **81**, 275 (1951).
- [7] J. Marshall, *Phys. Rev.* **86**, 685 (1952).
- [8] M. Danos, S. Geschwind, H. Lashinsky, and A. van Trier, *Phys. Rev.* **92**, 828 (1953).
- [9] P. D. Coleman and C. Enderby, *J. Appl. Phys.* **31**, 1695 (1960).
- [10] T. Takahashi, Y. Shibata, K. Ishi, M. Ikezawa, M. Oyamada, and Y. Kondo, *Phys. Rev. E* **62**, 8606 (2000).
- [11] N. Sei, T. Sakai, K. Hayakawa, T. Tanaka, Y. Hayakawa, K. Nakao, K. Nogami, and M. Inagaki, *Phys. Lett. A* **379**, 2399 (2015).
- [12] N. Sei and T. Takahashi, *Sci. Rep.* **7**, 17440 (2017).
- [13] A. P. Potylitsyn, S. Y. Gogolev, D. V. Karlovets, G. A. Naumenko, Y. A. Popov, M. V. Shevelev, and L. G. Sukhikh, in *Proceedings of IPAC'10* (JACoW, Geneva, 2010), pp. 1074–1076.
- [14] M. Bergamaschi, R. Kieffer, R. Jones, T. Lefevre, S. Mazzoni, M. Billing, J. Conway, J. Shanks, P. Karataev, and L. Bobb, in *Proceedings of International Particle Accelerator Conference (IPAC'17), Copenhagen, Denmark, 14–19 May, 2017*, International Particle Accelerator Conference No. 8 (JACoW, Geneva, 2017), pp. 400–403.
- [15] R. Kieffer, L. Bartnik, M. Bergamaschi, V. V. Bleko, M. Billing, L. Bobb, J. Conway, M. Forster, P. Karataev, A. S. Konkov, R. O. Jones, T. Lefevre, J. S. Markova, S. Mazzoni, Y. Padilla Fuentes, A. P. Potylitsyn, J. Shanks, and S. Wang, *Phys. Rev. Lett.* **121**, 054802 (2018).
- [16] I. E. Tamm and I. M. Frank, *Compt. Rend. Acad. Sci. URSS* **14**, 109 (1937).
- [17] I. E. Tamm, *J. Phys. USSR* **1**, 439 (1939).
- [18] E. S. Belonogaya, A. V. Tyukhtin, and S. N. Galyamin, *Phys. Rev. E* **87**, 043201 (2013).
- [19] E. S. Belonogaya, S. N. Galyamin, and A. V. Tyukhtin, *J. Opt. Soc. Am. B* **32**, 649 (2015).
- [20] S. N. Galyamin and A. V. Tyukhtin, *Phys. Rev. Lett.* **113**, 064802 (2014).
- [21] S. Galyamin, A. Tyukhtin, and V. Vorobev, *J. Instrum.* **13**, C02029 (2018).
- [22] A. Tyukhtin, V. Vorobev, E. Belonogaya, and S. Galyamin, *J. Instrum.* **13**, C02033 (2018).
- [23] A. V. Tyukhtin, V. V. Vorobev, S. N. Galyamin, and E. S. Belonogaya, *Phys. Rev. Accel. Beams* **22**, 012802 (2019).
- [24] A. V. Tyukhtin, S. N. Galyamin, and V. V. Vorobev, *Phys. Rev. A* **99**, 023810 (2019).
- [25] G. Toraldo di Francia, *Il Nuovo Cimento* **16**, 61 (1960).
- [26] R. Ulrich, *Z. Phys.* **194**, 180 (1966).
- [27] B. M. Bolotovskii, *Phys. Usp.* **4**, 781 (1962).
- [28] L. S. Bogdankevich and B. M. Bolotovskii, *JETP* **5**, 1157 (1957).
- [29] S. N. Galyamin, V. V. Vorobev, and A. V. Tyukhtin, *Phys. Rev. Accel. Beams* **22**, 083001 (2019).
- [30] S. N. Galyamin, V. V. Vorobev, and A. V. Tyukhtin, *Phys. Rev. Accel. Beams* **22**, 109901(E) (2019).
- [31] A. Z. Fradin, *Microwave Antennas* (Pergamon, Oxford, 1961).
- [32] L. B. Felsen and N. Marcuvitz, *Radiation and Scattering of Waves* (Wiley Interscience, Hoboken, 2003).
- [33] Y. A. Kravtsov and Y. I. Orlov, *Geometrical Optics of Inhomogeneous Media*, Springer Series on Wave Phenomena, Vol. 6 (Springer-Verlag, Berlin/Heidelberg, 1990).
- [34] V. A. Fok, *Electromagnetic Diffraction and Propagation Problems* (Pergamon Press, Oxford, 1965).
- [35] A. P. Prudnikov, Y. A. Brychkov, and O. I. Marichev, *Integrals and Series, Vol. 1, Elementary Functions* (Gordon & Breach Science Publications, New York, 1986).
- [36] M. Abramowitz and I. A. Stegun (eds.), *Handbook of Mathematical Functions: With Formulas, Graphs, and Mathematical Tables* (Dover Publications, New York, 1972).